

PARTICLES AND FIELDS • OPEN ACCESS

Measurement of the absolute branching fraction of $D^+ \rightarrow K^0 e^+ \nu_e$ via $K^0 \rightarrow \pi^0 \pi^{0*}$

To cite this article: M. Ablikim *et al* 2016 *Chinese Phys. C* **40** 113001

View the [article online](#) for updates and enhancements.

You may also like

- [GW190814: Gravitational Waves from the Coalescence of a 23 Solar Mass Black Hole with a 2.6 Solar Mass Compact Object](#)
R. Abbott, T. D. Abbott, S. Abraham et al.
- [Properties and Astrophysical Implications of the 150 \$M\$ Binary Black Hole Merger GW190521](#)
R. Abbott, T. D. Abbott, S. Abraham et al.
- [Study of BESIII trigger efficiencies with the 2018 \$J/\psi\$ data](#)
M. Ablikim, , M. N. Achasov et al.

Measurement of the absolute branching fraction of $D^+ \rightarrow \bar{K}^0 e^+ \nu_e$ via $\bar{K}^0 \rightarrow \pi^0 \pi^0^*$

M. Ablikim(麦迪娜)¹ M. N. Achasov^{9,e} X. C. Ai(艾小聪)¹ O. Albayrak⁵ M. Albrecht⁴ D. J. Ambrose⁴⁴ A. Amoroso^{49A,49C} F. F. An(安芬芬)¹ Q. An(安琪)^{46,a} J. Z. Bai(白景芝)¹ R. Baldini Ferroli^{20A} Y. Ban(班勇)³¹ D. W. Bennett¹⁹ J. V. Bennett⁵ M. Bertani^{20A} D. Bettoni^{21A} J. M. Bian(边渐鸣)⁴³ F. Bianchi^{49A,49C} E. Boger^{23,c} I. Boyko²³ R. A. Briere⁵ H. Cai(蔡浩)⁵¹ X. Cai(蔡啸)^{1,a} O. Cakir^{40A} A. Calcaterra^{20A} G. F. Cao(曹国富)¹ S. A. Cetin^{40B} J. F. Chang(常劲帆)^{1,a} G. Chelkov^{23,c,d} G. Chen(陈刚)¹ H. S. Chen(陈和生)¹ H. Y. Chen(陈海云)² J. C. Chen(陈江川)¹ M. L. Chen(陈玛丽)^{1,a} S. Chen(陈实)⁴¹ S. J. Chen(陈申见)²⁹ X. Chen(谌炫)^{1,a} X. R. Chen(陈旭荣)²⁶ Y. B. Chen(陈元柏)^{1,a} H. P. Cheng(程和平)¹⁷ X. K. Chu(褚新坤)³¹ G. Cibinetto^{21A} H. L. Dai(代洪亮)^{1,a} J. P. Dai(代建平)³⁴ A. Dbeyssi¹⁴ D. Dedovich²³ Z. Y. Deng(邓子艳)¹ A. Denig²² I. Denysenko²³ M. Destefanis^{49A,49C} F. De Mori^{49A,49C} Y. Ding(丁勇)²⁷ C. Dong(董超)³⁰ J. Dong(董静)^{1,a} L. Y. Dong(董燎原)¹ M. Y. Dong(董明义)^{1,a} Z. L. Dou(豆正磊)²⁹ S. X. Du(杜书先)⁵³ P. F. Duan(段鹏飞)¹ J. Z. Fan(范荆州)³⁹ J. Fang(方建)^{1,a} S. S. Fang(房双世)¹ X. Fang(方馨)^{46,a} Y. Fang(方易)¹ R. Farinelli^{21A,21B} L. Fava^{49B,49C} O. Fedorov²³ F. Feldbauer²² G. Felici^{20A} C. Q. Feng(封常青)^{46,a} E. Fioravanti^{21A} M. Fritsch^{14,22} C. D. Fu(傅成栋)¹ Q. Gao(高清)¹ X. L. Gao(高鑫磊)^{46,a} X. Y. Gao(高旭阳)² Y. Gao(高原宁)³⁹ Z. Gao(高榛)^{46,a} I. Garzia^{21A} K. Goetzen¹⁰ L. Gong(龚丽)³⁰ W. X. Gong(龚文煊)¹ W. Gradl²² M. Greco^{49A,49C} M. H. Gu(顾旻皓)^{1,a} Y. T. Gu(顾运厅)¹² Y. H. Guan(管颖慧)¹ A. Q. Guo(郭爱强)¹ L. B. Guo(郭立波)²⁸ R. P. Guo(郭如盼)¹ Y. Guo(郭玥)¹ Y. P. Guo(郭玉萍)²² Z. Haddadi²⁵ A. Hafner²² S. Han(韩爽)⁵¹ X. Q. Hao(郝喜庆)¹⁵ F. A. Harris⁴² K. L. He(何康林)¹ T. Held⁴ Y. K. Heng(衡月昆)^{1,a} Z. L. Hou(侯治龙)¹ C. Hu(胡琛)²⁸ H. M. Hu(胡海明)¹ J. F. Hu(胡继峰)^{49A,49C} T. Hu(胡涛)^{1,a} Y. Hu(胡誉)¹ G. S. Huang(黄光顺)^{46,a} J. S. Huang(黄金书)¹⁵ X. T. Huang(黄性涛)³³ X. Z. Huang(黄晓忠)²⁹ Y. Huang(黄勇)²⁹ Z. L. Huang(黄智玲)²⁷ T. Hussain⁴⁸ Q. Ji(纪全)¹ Q. P. Ji(姬清平)³⁰ X. B. Ji(季晓斌)¹ X. L. Ji(季筱璐)^{1,a} L. W. Jiang(姜鲁文)⁵¹ X. S. Jiang(江晓山)^{1,a} X. Y. Jiang(蒋兴雨)³⁰ J. B. Jiao(焦健斌)³³ Z. Jiao(焦铮)¹⁷ D. P. Jin(金大鹏)^{1,a} S. Jin(金山)¹ T. Johansson⁵⁰ A. Julin⁴³ N. Kalantar-Nayestanaki²⁵ X. L. Kang(康晓琳)¹ X. S. Kang(康晓坤)³⁰ M. Kavatsyuk²⁵ B. C. Ke(柯百谦)⁵ P. Kiese²² R. Kliemt¹⁴ B. Kloss²² O. B. Kolcu^{40B,h} B. Kopf⁴ M. Kornicer⁴² A. Kupsc⁵⁰ W. Kühn²⁴ J. S. Lange²⁴ M. Lara¹⁹ P. Larin¹⁴ C. Leng^{49C} C. Li(李翠)⁵⁰ Cheng Li(李澄)^{46,a} D. M. Li(李德民)⁵³ F. Li(李飞)^{1,a} F. Y. Li(李峰云)³¹ G. Li(李刚)¹ H. B. Li(李海波)¹ H. J. Li(李惠静)¹ J. C. Li(李家才)¹ Jin Li(李瑾)³² K. Li(李康)¹³ K. Li(李科)³³ Lei Li(李蕾)³ P. R. Li(李培荣)⁴¹ Q. Y. Li(李启云)³³ T. Li(李腾)³³ W. D. Li(李卫东)¹ W. G. Li(李卫国)¹ X. L. Li(李晓玲)³³ X. N. Li(李小男)^{1,a} X. Q. Li(李学潜)³⁰ Y. B. Li(李郁博)² Z. B. Li(李志兵)³⁸ H. Liang(梁昊)^{46,a} Y. F. Liang(梁勇飞)³⁶ Y. T. Liang(梁羽铁)²⁴ G. R. Liao(廖广睿)¹¹ D. X. Lin(林德旭)¹⁴ B. Liu(刘冰)³⁴ B. J. Liu(刘北江)¹ C. X. Liu(刘春秀)¹ D. Liu(刘栋)^{46,a} F. H. Liu(刘福虎)³⁵ Fang Liu(刘芳)¹ Feng Liu(刘峰)⁶ H. B. Liu(刘宏邦)¹² H. H. Liu(刘汇慧)¹⁶ H. H. Liu(刘欢欢)¹

Received 3 May 2016, Revised 29 June 2016

* Supported by National Key Basic Research Program of China (2009CB825204, 2015CB856700), National Natural Science Foundation of China (NSFC) (10935007, 11125525, 11235011, 11305180, 11322544, 11335008, 11425524, 11475123), Chinese Academy of Sciences (CAS) Large-Scale Scientific Facility Program, CAS Center for Excellence in Particle Physics (CCEPP), Collaborative Innovation Center for Particles and Interactions (CICPI), Joint Large-Scale Scientific Facility Funds of NSFC and CAS (11179007, U1232201, U1332201, U1532101), CAS (KJCX2-YW-N29, KJCX2-YW-N45), 100 Talents Program of CAS, National 1000 Talents Program of China, IN-PAC and Shanghai Key Laboratory for Particle Physics and Cosmology, German Research Foundation DFG (Collaborative Research Center CRC-1044), Istituto Nazionale di Fisica Nucleare, Italy, Koninklijke Nederlandse Akademie van Wetenschappen (KNAW) (530-4CDP03), Ministry of Development of Turkey (DPT2006K-120470), National Natural Science Foundation of China (NSFC) (11405046, U1332103), Russian Foundation for Basic Research (14-07-91152), Swedish Research Council, U. S. Department of Energy (DE-FG02-04ER41291, DE-FG02-05ER41374, DE-SC0012069, DESC0010118), U.S. National Science Foundation, University of Groningen (RuG) and Helmholtzzentrum fuer Schwerionenforschung GmbH (GSI), Darmstadt, WCU Program of National Research Foundation of Korea (R32-2008-000-10155-0).



Content from this work may be used under the terms of the Creative Commons Attribution 3.0 licence. Any further distribution of this work must maintain attribution to the author(s) and the title of the work, journal citation and DOI. Article funded by SCOAP³ and published under licence by Chinese Physical Society and the Institute of High Energy Physics of the Chinese Academy of Sciences and the Institute of Modern Physics of the Chinese Academy of Sciences and IOP Publishing Ltd

H. M. Liu(刘怀民)¹ J. Liu(刘杰)¹ J. B. Liu(刘建北)^{46,a} J. P. Liu(刘觉平)⁵¹ J. Y. Liu(刘晶译)¹
 K. Liu(刘凯)³⁹ K. Y. Liu(刘魁勇)²⁷ L. D. Liu(刘兰雕)³¹ P. L. Liu(刘佩莲)^{1,a} Q. Liu(刘倩)⁴¹
 S. B. Liu(刘树彬)^{46,a} X. Liu(刘翔)²⁶ Y. B. Liu(刘玉斌)³⁰ Z. A. Liu(刘振安)^{1,a} Zhiqing Liu(刘智青)²²
 H. Loehner²⁵ X. C. Lou(娄辛丑)^{1,a,g} H. J. Lü(吕海江)¹⁷ J. G. Lü(吕军光)^{1,a} Y. Lu(卢宇)¹
 Y. P. Lu(卢云鹏)^{1,a} C. L. Luo(罗成林)²⁸ M. X. Luo(罗民兴)⁵² T. Luo⁴² X. L. Luo(罗小兰)^{1,a}
 X. R. Lü(吕晓睿)⁴¹ F. C. Ma(马凤才)²⁷ H. L. Ma(马海龙)¹ L. L. Ma(马连良)³³ M. M. Ma(马明明)¹
 Q. M. Ma(马秋梅)¹ T. Ma(马天)¹ X. N. Ma(马旭宁)³⁰ X. Y. Ma(马骁妍)^{1,a} Y. M. Ma(马玉明)³³
 F. E. Maas¹⁴ M. Maggiora^{49A,49C} Y. J. Mao(冒亚军)³¹ Z. P. Mao(毛泽普)¹ S. Marcello^{49A,49C}
 J. G. Messchendorp²⁵ J. Min(闵建)^{1,a} T. J. Min(闵天觉)¹ R. E. Mitchell¹⁹ X. H. Mo(莫晓虎)^{1,a}
 Y. J. Mo(莫玉俊)⁶ C. Morales Morales¹⁴ N. Yu. Muchnoi^{9,e} H. Muramatsu⁴³ Y. Nefedov²³
 F. Nerling¹⁴ I. B. Nikolaev^{9,e} Z. Ning(宁哲)^{1,a} S. Nisar⁸ S. L. Niu(牛顺利)^{1,a} X. Y. Niu(牛讯伊)¹
 S. L. Olsen(馬鵬)³² Q. Ouyang(欧阳群)^{1,a} S. Pacetti^{20B} Y. Pan(潘越)^{46,a} P. Patteri^{20A} M. Pelizaesus⁴
 H. P. Peng(彭海平)^{46,a} K. Peters^{10,i} J. Pettersson⁵⁰ J. L. Ping(平加伦)²⁸ R. G. Ping(平荣刚)¹
 R. Poling⁴³ V. Prasad¹ H. R. Qi(漆红荣)² M. Qi(祁鸣)²⁹ S. Qian(钱森)^{1,a} C. F. Qiao(乔从丰)⁴¹
 L. Q. Qin(秦丽清)³³ N. Qin(覃拈)⁵¹ X. S. Qin(秦小帅)¹ Z. H. Qin(秦中华)^{1,a} J. F. Qiu(邱进发)¹
 K. H. Rashid⁴⁸ C. F. Redmer²² M. Ripka²² G. Rong(荣刚)¹ Ch. Rosner¹⁴ X. D. Ruan(阮向东)¹²
 A. Sarantsev^{23,f} M. Savrié^{21B} K. Schoenning⁵⁰ S. Schumann²² W. Shan(单葳)³¹ M. Shao(邵明)^{46,a}
 C. P. Shen(沈成平)² P. X. Shen(沈培迅)³⁰ X. Y. Shen(沈肖雁)¹ H. Y. Sheng(盛华义)¹ M. Shi(施萌)¹
 W. M. Song(宋维民)¹ X. Y. Song(宋欣颖)¹ S. Sosio^{49A,49C} S. Spataro^{49A,49C} G. X. Sun(孙功星)¹
 J. F. Sun(孙俊峰)¹⁵ S. S. Sun(孙胜森)¹ X. H. Sun(孙新华)¹ Y. J. Sun(孙勇杰)^{46,a} Y. Z. Sun(孙永昭)¹
 Z. J. Sun(孙志嘉)^{1,a} Z. T. Sun(孙振田)¹⁹ C. J. Tang(唐昌建)³⁶ X. Tang(唐晓)¹ I. Tapan^{40C}
 E. H. Thorndike⁴⁴ M. Tiemens²⁵ M. Ullrich²⁴ I. Uman^{40D} G. S. Varner⁴² B. Wang(王斌)³⁰
 B. L. Wang(王滨龙)⁴¹ D. Wang(王东)³¹ D. Y. Wang(王大勇)³¹ K. Wang(王科)^{1,a} L. L. Wang(王亮亮)¹
 L. S. Wang(王灵淑)¹ M. Wang(王萌)³³ P. Wang(王平)¹ P. L. Wang(王佩良)¹ W. Wang(王炜)^{1,a}
 W. P. Wang(王维平)^{46,a} X. F. Wang(王雄飞)³⁹ Y. Wang(王越)³⁷ Y. D. Wang(王雅迪)¹⁴
 Y. F. Wang(王贻芳)^{1,a} Y. Q. Wang(王亚乾)²² Z. Wang(王铮)^{1,a} Z. G. Wang(王志刚)^{1,a}
 Z. H. Wang(王志宏)⁴⁶ Z. Y. Wang(王至勇)¹ Z. Y. Wang(王宗源)¹ T. Weber²² D. H. Wei(魏代会)¹¹
 P. Weidenkaff²² S. P. Wen(文硕频)¹ U. Wiedner⁴ M. Wolke⁵⁰ L. H. Wu(伍灵慧)¹ L. J. Wu(吴连近)¹
 Z. Wu(吴智)^{1,a} L. Xia(夏磊)^{46,a} L. G. Xia(夏力钢)³⁹ Y. Xia(夏宇)¹⁸ D. Xiao(肖栋)¹ H. Xiao(肖浩)⁴⁷
 Z. J. Xiao(肖振军)²⁸ Y. G. Xie(谢宇广)^{1,a} Q. L. Xiu(修青磊)^{1,a} G. F. Xu(许国发)¹ J. J. Xu(徐静静)¹
 L. Xu(徐雷)¹ Q. J. Xu(徐庆君)¹³ Q. N. Xu(徐庆年)⁴¹ X. P. Xu(徐新平)³⁷ L. Yan(严亮)^{49A,49C}
 W. B. Yan(鄢文标)^{46,a} W. C. Yan(闫文成)^{46,a} Y. H. Yan(颜永红)¹⁸ H. J. Yang(杨海军)³⁴
 H. X. Yang(杨洪勋)¹ L. Yang(杨柳)⁵¹ Y. X. Yang(杨永翎)¹¹ M. Ye(叶梅)^{1,a} M. H. Ye(叶铭汉)⁷
 J. H. Yin(殷俊昊)¹ B. X. Yu(俞伯祥)^{1,a} C. X. Yu(喻纯旭)³⁰ J. S. Yu(俞洁晟)²⁶ C. Z. Yuan(苑长征)¹
 W. L. Yuan(袁文龙)²⁹ Y. Yuan(袁野)¹ A. Yuncu^{40B,b} A. A. Zafar⁴⁸ A. Zallo^{20A} Y. Zeng(曾云)¹⁸
 Z. Zeng(曾哲)^{46,a} B. X. Zhang(张丙新)¹ B. Y. Zhang(张炳云)^{1,a} C. Zhang(张驰)²⁹ C. C. Zhang(张长春)¹
 D. H. Zhang(张达华)¹ H. H. Zhang(张宏浩)³⁸ H. Y. Zhang(章红宇)^{1,a} J. Zhang(张晋)¹
 J. J. Zhang(张佳佳)¹ J. L. Zhang(张杰磊)¹ J. Q. Zhang(张敬庆)¹ J. W. Zhang(张家文)^{1,a}
 J. Y. Zhang(张建勇)¹ J. Z. Zhang(张景芝)¹ K. Zhang(张坤)¹ L. Zhang(张磊)¹ S. Q. Zhang(张士权)³⁰
 X. Y. Zhang(张学尧)³³ Y. Zhang(张瑶)¹ Y. H. Zhang(张银鸿)^{1,a} Y. N. Zhang(张宇宁)⁴¹
 Y. T. Zhang(张亚腾)^{46,a} Yu Zhang(张宇)⁴¹ Z. H. Zhang(张正好)⁶ Z. P. Zhang(张子平)⁴⁶
 Z. Y. Zhang(张振宇)⁵¹ G. Zhao(赵光)¹ J. W. Zhao(赵京伟)^{1,a} J. Y. Zhao(赵静宜)¹ J. Z. Zhao(赵京周)^{1,a}
 Lei Zhao(赵雷)^{46,a} Ling Zhao(赵玲)¹ M. G. Zhao(赵明刚)³⁰ Q. Zhao(赵强)¹ Q. W. Zhao(赵庆旺)¹
 S. J. Zhao(赵书俊)⁵³ T. C. Zhao(赵天池)¹ Y. B. Zhao(赵豫斌)^{1,a} Z. G. Zhao(赵政国)^{46,a}
 A. Zhemchugov^{23,c} B. Zheng(郑波)⁴⁷ J. P. Zheng(郑建平)^{1,a} W. J. Zheng(郑文静)³³ Y. H. Zheng(郑阳恒)⁴¹
 B. Zhong(钟彬)²⁸ L. Zhou(周莉)^{1,a} X. Zhou(周详)⁵¹ X. K. Zhou(周晓康)^{46,a} X. R. Zhou(周小蓉)^{46,a}
 X. Y. Zhou(周兴玉)¹ K. Zhu(朱凯)¹ K. J. Zhu(朱科军)^{1,a} S. Zhu(朱帅)¹ S. H. Zhu(朱世海)⁴⁵
 X. L. Zhu(朱相雷)³⁹ Y. C. Zhu(朱莹春)^{46,a} Y. S. Zhu(朱永生)¹ Z. A. Zhu(朱自安)¹ J. Zhuang(庄建)^{1,a}
 L. Zotti^{49A,49C} B. S. Zou(邹冰松)¹ J. H. Zou(邹佳恒)¹

(BESIII Collaboration)

¹ Institute of High Energy Physics, Beijing 100049, China² Beihang University, Beijing 100191, China³ Beijing Institute of Petrochemical Technology, Beijing 102617, China⁴ Bochum Ruhr-University, D-44780 Bochum, Germany⁵ Carnegie Mellon University, Pittsburgh, Pennsylvania 15213, USA

- ⁶ Central China Normal University, Wuhan 430079, China
⁷ China Center of Advanced Science and Technology, Beijing 100190, China
⁸ COMSATS Institute of Information Technology, Lahore, Defence Road, Off Raiwind Road, 54000 Lahore, Pakistan
⁹ G.I. Budker Institute of Nuclear Physics SB RAS (BINP), Novosibirsk 630090, Russia
¹⁰ GSI Helmholtzcentre for Heavy Ion Research GmbH, D-64291 Darmstadt, Germany
¹¹ Guangxi Normal University, Guilin 541004, China
¹² Guangxi University, Nanning 530004, China
¹³ Hangzhou Normal University, Hangzhou 310036, China
¹⁴ Helmholtz Institute Mainz, Johann-Joachim-Becher-Weg 45, D-55099 Mainz, Germany
¹⁵ Henan Normal University, Xinxiang 453007, China
¹⁶ Henan University of Science and Technology, Luoyang 471003, China
¹⁷ Huangshan College, Huangshan 245000, China
¹⁸ Hunan University, Changsha 410082, China
¹⁹ Indiana University, Bloomington, Indiana 47405, USA
²⁰ (A)INFN Laboratori Nazionali di Frascati, I-00044, Frascati, Italy; (B)INFN and University of Perugia, I-06100, Perugia, Italy
²¹ (A)INFN Sezione di Ferrara, I-44122, Ferrara, Italy; (B)University of Ferrara, I-44122, Ferrara, Italy
²² Johannes Gutenberg University of Mainz, Johann-Joachim-Becher-Weg 45, D-55099 Mainz, Germany
²³ Joint Institute for Nuclear Research, 141980 Dubna, Moscow region, Russia
²⁴ Justus-Liebig-Universitaet Giessen, II. Physikalisches Institut, Heinrich-Buff-Ring 16, D-35392 Giessen, Germany
²⁵ KVI-CART, University of Groningen, NL-9747 AA Groningen, The Netherlands
²⁶ Lanzhou University, Lanzhou 730000, China
²⁷ Liaoning University, Shenyang 110036, China
²⁸ Nanjing Normal University, Nanjing 210023, China
²⁹ Nanjing University, Nanjing 210093, China
³⁰ Nankai University, Tianjin 300071, China
³¹ Peking University, Beijing 100871, China
³² Seoul National University, Seoul, 151-747 Korea
³³ Shandong University, Jinan 250100, China
³⁴ Shanghai Jiao Tong University, Shanghai 200240, China
³⁵ Shanxi University, Taiyuan 030006, China
³⁶ Sichuan University, Chengdu 610064, China
³⁷ Soochow University, Suzhou 215006, China
³⁸ Sun Yat-Sen University, Guangzhou 510275, China
³⁹ Tsinghua University, Beijing 100084, China
⁴⁰ (A)Ankara University, 06100 Tandogan, Ankara, Turkey; (B)Istanbul Bilgi University, 34060 Eyup, Istanbul, Turkey; (C)Uludag University, 16059 Bursa, Turkey; (D)Near East University, Nicosia, North Cyprus, Mersin 10, Turkey
⁴¹ University of Chinese Academy of Sciences, Beijing 100049, China
⁴² University of Hawaii, Honolulu, Hawaii 96822, USA
⁴³ University of Minnesota, Minneapolis, Minnesota 55455, USA
⁴⁴ University of Rochester, Rochester, New York 14627, USA
⁴⁵ University of Science and Technology Liaoning, Anshan 114051, China
⁴⁶ University of Science and Technology of China, Hefei 230026, China
⁴⁷ University of South China, Hengyang 421001, China
⁴⁸ University of the Punjab, Lahore-54590, Pakistan
⁴⁹ (A)University of Turin, I-10125, Turin, Italy; (B)University of Eastern Piedmont, I-15121, Alessandria, Italy; (C)INFN, I-10125, Turin, Italy
⁵⁰ Uppsala University, Box 516, SE-75120 Uppsala, Sweden
⁵¹ Wuhan University, Wuhan 430072, China
⁵² Zhejiang University, Hangzhou 310027, China
⁵³ Zhengzhou University, Zhengzhou 450001, China
^a Also at State Key Laboratory of Particle Detection and Electronics, Beijing 100049, Hefei 230026, China
^b Also at Bogazici University, 34342 Istanbul, Turkey
^c Also at the Moscow Institute of Physics and Technology, Moscow 141700, Russia
^d Also at the Functional Electronics Laboratory, Tomsk State University, Tomsk, 634050, Russia
^e Also at the Novosibirsk State University, Novosibirsk, 630090, Russia
^f Also at the NRC "Kurchatov Institute, PNPI, 188300, Gatchina, Russia
^g Also at University of Texas at Dallas, Richardson, Texas 75083, USA
^h Also at Istanbul Arel University, 34295 Istanbul, Turkey
ⁱ Also at Goethe University Frankfurt, 60323 Frankfurt am Main, Germany

Abstract: By analyzing 2.93 fb^{-1} data collected at the center-of-mass energy $\sqrt{s} = 3.773 \text{ GeV}$ with the BESIII detector, we measure the absolute branching fraction of the semileptonic decay $D^+ \rightarrow \bar{K}^0 e^+ \nu_e$ to be $\mathcal{B}(D^+ \rightarrow \bar{K}^0 e^+ \nu_e) = (8.59 \pm 0.14 \pm 0.21)\%$ using $\bar{K}^0 \rightarrow K_S^0 \rightarrow \pi^0 \pi^0$, where the first uncertainty is statistical and the second systematic. Our result is consistent with previous measurements within uncertainties..

Keywords: charmed mesons, semileptonic decays, absolute branching fraction, BESIII/BEPCII

PACS: 13.20.Fc, 14.40.Lb **DOI:** 10.1088/1674-1137/40/11/113001

1 Introduction

The study of semileptonic decays of D mesons can shed light on the strong and weak effects in charmed meson decays. The absolute branching fraction \mathcal{B} of the semileptonic decay $D^+ \rightarrow \bar{K}^0 e^+ \nu_e$ can be used to extract the form factor $f_+^K(0)$ of the hadronic weak current or the quark mixing matrix element $|V_{cs}|$ [1], which are important to calibrate the lattice quantum chromodynamics calculation on $f_+^K(0)$ and to test the unitarity of the quark mixing matrix. In addition, the measured $\mathcal{B}(D^+ \rightarrow \bar{K}^0 e^+ \nu_e)$ can also be used to test isospin symmetry in the $D^+ \rightarrow \bar{K}^0 e^+ \nu_e$ and $D^0 \rightarrow K^- e^+ \nu_e$ decays [2–5]. Therefore, improving the measurement precision of $\mathcal{B}(D^+ \rightarrow \bar{K}^0 e^+ \nu_e)$ will be helpful to better understand the D decay mechanisms.

Measurements of $\mathcal{B}(D^+ \rightarrow \bar{K}^0 e^+ \nu_e)$ via $\bar{K}^0 \rightarrow K_S^0 \rightarrow \pi^+ \pi^-$ have been performed by the MARKIII, BES, CLEO and BESIII Collaborations [2–6]. Recently, a measurement of $\mathcal{B}(D^+ \rightarrow \bar{K}_L^0 e^+ \nu_e)$ has been carried out by the BESIII Collaboration [7]. However, no measurement of $\mathcal{B}(D^+ \rightarrow \bar{K}^0 e^+ \nu_e)$ using $\bar{K}^0 \rightarrow K_S^0 \rightarrow \pi^0 \pi^0$ has been reported so far. As a first step, we present in this paper a measurement of $\mathcal{B}(D^+ \rightarrow \bar{K}^0 e^+ \nu_e)$ using $\bar{K}^0 \rightarrow K_S^0 \rightarrow \pi^0 \pi^0$, based on an analysis of 2.93 fb^{-1} of $e^+ e^-$ collision data [8, 9] accumulated at the center-of-mass energy $\sqrt{s} = 3.773 \text{ GeV}$ with the BESIII detector [10]. Since the $f_+^K(0)|V_{cs}|$ measurement with the $D^0 \rightarrow K^- e^+ \nu_e$ decay has achieved an accuracy of about 0.6% in our previous work [11], this analysis only aims to measure the absolute branching fraction for $D^+ \rightarrow \bar{K}^0 e^+ \nu_e$.

2 BESIII detector and Monte Carlo

The BESIII detector is a cylindrical detector with solid-angle 93% of 4π that operates at the BEPCII collider. It consists of several main components. A 43-layer main drift chamber (MDC) surrounding the beam pipe performs precise determinations of charged particle trajectories and provides ionization energy loss (dE/dx) measurements that are used for charged particle identification (PID). An array of time-of-flight counters (TOF) is located radially outside the MDC and provides additional charged particle identification information. A CsI(Tl) electromagnetic calorimeter (EMC) surrounds the TOF and is used to measure the energies of photons and electrons. A solenoidal superconducting magnet located outside the EMC provides a 1 T magnetic field in the central tracking region of the detector. The iron flux return of the magnet is instrumented with about 1272 m^2 of resistive plate muon counters (MUC) arranged in nine layers in the barrel and eight layers in the endcaps that are used to identify muons with momentum greater than $0.5 \text{ GeV}/c$. More details about the BESIII detector are described in Ref. [10].

A GEANT4-based [12] Monte Carlo (MC) simulation software, which includes the geometric description and a simulation of the response of the detector, is used to determine the detection efficiency and to estimate the potential backgrounds. An inclusive MC sample, which includes generic $\psi(3770)$ decays, initial state radiation (ISR) production of $\psi(3686)$ and J/ψ , QED ($e^+ e^- \rightarrow e^+ e^-$, $\mu^+ \mu^-$, $\tau^+ \tau^-$) and $q\bar{q}$ ($q = u, d, s$) continuum processes, is produced at $\sqrt{s} = 3.773 \text{ GeV}$. The MC events of $\psi(3770)$ decays are produced by a combination of the MC generators KKMC [13, 14] and PHOTOS [15], in which the effects of ISR [16] and Final State Radiation (FSR) are considered. The known decay modes of charmonium states are generated using EvtGen [17, 18] with the branching fractions taken from the Particle Data Group (PDG) [19], and the unknown decay modes are generated using LundCharm [20]. The $D^+ \rightarrow \bar{K}^0 e^+ \nu_e$ signal is modeled by the modified pole model [21].

3 Measurement

3.1 Single tag D^- mesons

With a mass of 3.773 GeV just above the open charm threshold, the $\psi(3770)$ resonance decays predominately into $D^0 \bar{D}^0$ or $D^+ D^-$ meson pairs. In each event, if a D^- meson can be fully reconstructed via its decay into hadrons (in the following called the single tag (ST) D^-), there must be a recoiling D^+ meson. Using a double tag technique which was first employed by the MARKIII Collaboration [22], we can measure the absolute branching fraction of the $D^+ \rightarrow \bar{K}^0 e^+ \nu_e$ decay. Throughout the paper, charge conjugation is implied.

The ST D^- mesons are reconstructed using six hadronic decay modes: $K^+ \pi^- \pi^-$, $K_S^0 \pi^-$, $K^+ \pi^- \pi^- \pi^0$, $K_S^0 \pi^- \pi^0$, $K_S^0 \pi^+ \pi^- \pi^-$ and $K^+ K^- \pi^-$. The daughter particles K_S^0 and π^0 are reconstructed via $K_S^0 \rightarrow \pi^+ \pi^-$ and $\pi^0 \rightarrow \gamma\gamma$, respectively.

All charged tracks are required to be reconstructed within the good MDC acceptance $|\cos\theta| < 0.93$, where θ is the polar angle of the track with respect to the positron beam direction. All tracks except those from K_S^0 decays are required to originate from the interaction region defined as $V_{xy} < 1.0 \text{ cm}$ and $|V_z| < 10.0 \text{ cm}$. Here, V_{xy} and $|V_z|$ are the distances of closest approach to the Interaction Point (IP) of the reconstructed track in the plane transverse to and along the beam direction, respectively. For PID of charged particles [23], we combine the dE/dx and TOF information to calculate Confidence Levels for the pion and kaon hypotheses (CL_π and CL_K). A charged track is taken as kaon (pion) if it has $CL_K > CL_\pi$ ($CL_\pi > CL_K$).

The charged tracks from K_S^0 decays are required to satisfy $|V_z| < 20.0 \text{ cm}$. The two oppositely charged tracks, which are assumed as $\pi^+ \pi^-$ without PID, are

constrained to originate from a common vertex. A $\pi^+\pi^-$ combination is considered as a K_S^0 candidate if its invariant mass lies in the mass window $|M_{\pi^+\pi^-} - M_{K_S^0}| < 12 \text{ MeV}/c^2$, where $M_{K_S^0}$ is the nominal K_S^0 mass [24]. The $\pi^+\pi^-$ combinations with $L/\sigma_L > 2$ are retained, where σ_L is the uncertainty of the K_S^0 reconstructed decay length L .

Photon candidates are selected by using the EMC information. The shower time is required to be within 700 ns of the event start time, which is the interval of the trigger start time to the real collision time [25]. The shower energy is required to be greater than 25 (50) MeV in the barrel (endcap) region. The opening angle between the candidate shower and the closest charged track is required to be greater than 10° . A $\gamma\gamma$ combination is considered as a π^0 candidate if its invariant mass falls in $(0.115, 0.150) \text{ GeV}/c^2$. To obtain better mass resolution for the D^- candidates, the $\gamma\gamma$ invariant mass is constrained to the π^0 nominal mass [24] via a kinematic fit.

To suppress combinatorial backgrounds, we define the variable $\Delta E = E_{mK_n\pi} - E_{\text{beam}}$, which is the difference between the measured energy of the $mK_n\pi$ ($m = 1, 2; n = 1, 2, 3$) combination ($E_{mK_n\pi}$) and the beam energy (E_{beam}). For each ST mode, if there is more than

one $mK_n\pi$ combination satisfying the above selection criteria, only the one with the minimum $|\Delta E|$ is kept. The ΔE is required to be within $(-25, +25) \text{ MeV}$ for the $K^+\pi^-\pi^-$, $K_S^0\pi^-$, $K_S^0\pi^+\pi^-\pi^-$ and $K^+K^-\pi^-$ combinations, and be within $(-55, +40) \text{ MeV}$ for the $K^+\pi^-\pi^-\pi^0$ and $K_S^0\pi^-\pi^0$ combinations.

To measure the yield of ST D^- mesons, we perform maximum likelihood fits to the spectra of the beam energy constrained masses $M_{\text{BC}} = \sqrt{E_{\text{beam}}^2/c^4 - |\vec{p}_{mK_n\pi}|^2/c^2}$ of the accepted $mK_n\pi$ combinations, as shown in Fig. 1. Here, $\vec{p}_{mK_n\pi}$ is the measured momentum of the $mK_n\pi$ combination. In the fits, the D^- signal is modeled by the MC simulated M_{BC} distribution convolved with a double Gaussian function, and the combinatorial background is described by an ARGUS function [26]. The parameters of the double Gaussian function and the ARGUS function are float. The candidates in the ST D^- signal region defined as $(1.863, 1.877) \text{ GeV}/c^2$ are kept for further analysis. Single-tag reconstruction efficiencies ϵ_{ST} are estimated by analyzing the inclusive MC sample. The ST yields N_{ST} and the ST efficiencies are summarized in Table 1. The total ST yield is $N_{\text{ST}}^{\text{tot}} = 1522474 \pm 2215$, where the uncertainty is the quadratic sum of the uncertainties from all the M_{BC} fits.

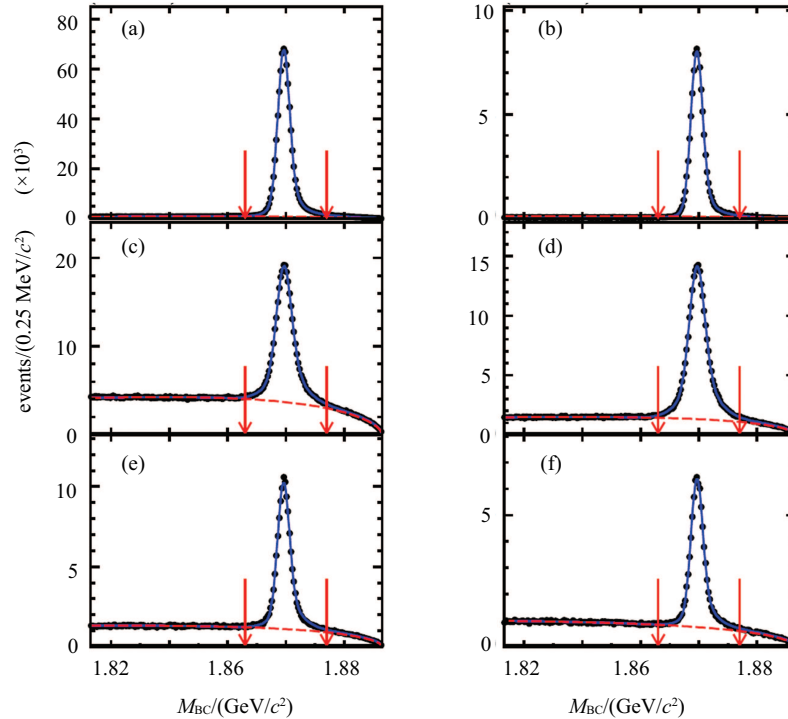


Fig. 1. (color online) Fits to the M_{BC} spectra of the (a) $K^+\pi^-\pi^-$, (b) $K_S^0\pi^-\pi^0$, (c) $K^+\pi^-\pi^-\pi^0$, (d) $K_S^0\pi^-\pi^0$, (e) $K_S^0\pi^+\pi^-\pi^-$ and (f) $K^+K^-\pi^-$ combinations. The dots with error bars are data, the blue solid curves are the fit results, the red dashed curves are the fitted backgrounds and the pair of red arrows in each sub-figure denote the ST D^- signal region.

Table 1. Summary of the ST yields (N_{ST}^i), the ST and DT efficiencies (ϵ_{ST}^i and ϵ_{DT}^i), and the reconstruction efficiencies of $D^+ \rightarrow \bar{K}^0 e^+ \nu_e$ ($\epsilon_{D^+ \rightarrow \bar{K}^0 e^+ \nu_e}^i$). The efficiencies do not include the branching fractions for $K_S^0 \rightarrow \pi^+ \pi^-$ (used in the reconstruction of ST D^- mesons), $\bar{K}^0 \rightarrow \pi^0 \pi^0$ and $\pi^0 \rightarrow \gamma\gamma$. The uncertainties are statistical only. The index i represents the i th ST mode.

ST mode i	N_{ST}^i	ϵ_{ST}^i (%)	ϵ_{DT}^i (%)	$\epsilon_{D^+ \rightarrow \bar{K}^0 e^+ \nu_e}^i$ (%)
$D^- \rightarrow K^+ \pi^- \pi^-$	782669±990	50.61±0.06	13.39±0.07	26.45±0.14
$D^- \rightarrow K_S^0 \pi^-$	91345±320	50.41±0.17	13.81±0.22	27.40±0.44
$D^- \rightarrow K^+ \pi^- \pi^- \pi^0$	251008±1135	26.74±0.09	6.23±0.06	23.29±0.25
$D^- \rightarrow K_S^0 \pi^- \pi^0$	215364±1238	27.29±0.07	6.88±0.07	25.21±0.28
$D^- \rightarrow K_S^0 \pi^+ \pi^- \pi^-$	113054±889	28.31±0.12	6.74±0.10	23.79±0.37
$D^- \rightarrow K^+ K^- \pi^-$	69034±460	40.83±0.24	10.54±0.20	25.81±0.50

3.2 Double tag events

In the system recoiling against the ST D^- mesons, the $D^+ \rightarrow \bar{K}^0 e^+ \nu_e$ candidates, called the double tag (DT) events, are selected via $\bar{K}^0 \rightarrow K_S^0 \rightarrow \pi^0 \pi^0$. It is required that there be at least four good photons and only one good charged track that have not been used in the ST selection. The good charged track, photons and π^0 mesons are selected using the same criteria as those used in the ST selection. If there are multiple $\pi^0 \pi^0$ combinations satisfying these selection criteria, only the combination with the minimum value of $\chi_1^2(\pi^0 \rightarrow \gamma\gamma) + \chi_2^2(\pi^0 \rightarrow \gamma\gamma)$ is retained, where the χ_1^2 and χ_2^2 are the chi-squares of the mass constrained fits on $\pi^0 \rightarrow \gamma\gamma$. A $\pi^0 \pi^0$ combination is considered as a \bar{K}^0 candidate if its invariant mass falls in (0.45, 0.51) GeV/ c^2 . For electron PID, we combine the dE/dx , TOF and EMC information to calculate Confidence Levels for the electron, pion and kaon hypotheses (CL_e , CL_π and CL_K), respectively. The electron candidate is required to have $CL_e > 0.001$ and $CL_e/(CL_e + CL_\pi + CL_K) > 0.8$, and to have a charge opposite to the ST D^- meson. To partially recover the effects of FSR and bremsstrahlung, the four-momenta of photon(s) within 5° of the initial electron direction are added to the electron four-momentum measured by the MDC. To suppress the backgrounds associated with fake photon(s), we require that the maximum energy ($E_{\max}^{\text{extra } \gamma}$) of any of the extra photons, which have not been used in the DT selection, be less than 300 MeV.

In order to obtain the information of the missing neutrino, we define the kinematic quantity

$$U_{\text{miss}} \equiv E_{\text{miss}} - |\vec{p}_{\text{miss}}|, \quad (1)$$

where E_{miss} and $|\vec{p}_{\text{miss}}|$ are the total energy and momentum of the missing particle in the event, respectively. E_{miss} is calculated by

$$E_{\text{miss}} = E_{\text{beam}} - E_{\bar{K}^0} - E_{e^+}, \quad (2)$$

where $E_{\bar{K}^0}$ and E_{e^+} are the energies carried by \bar{K}^0 and e^+ , respectively. $|\vec{p}_{\text{miss}}|$ is calculated by

$$|\vec{p}_{\text{miss}}| = |\vec{p}_{D^+} - \vec{p}_{\bar{K}^0} - \vec{p}_{e^+}|, \quad (3)$$

where \vec{p}_{D^+} , $\vec{p}_{\bar{K}^0}$ and \vec{p}_{e^+} are the momenta of D^+ , \bar{K}^0 and e^+ , respectively. To obtain better U_{miss} resolution, \vec{p}_{D^+} is constrained by

$$\vec{p}_{D^+} = -\hat{p}_{D_{ST}^-} \sqrt{E_{\text{beam}}^2 - m_{D^+}^2}, \quad (4)$$

where $\hat{p}_{D_{ST}^-}$ is the momentum direction of the ST D^- meson and m_{D^+} is the D^+ nominal mass [24].

To determine the number of DT events, we perform a maximum likelihood fit to the U_{miss} distribution of the accepted DT candidates, as shown in Fig. 2. In the fit, the DT signal and the combinatorial background are modeled by the MC simulated U_{miss} shapes, respectively. From the fit, we obtain the DT yield in data as

$$N_{DT} = 5013 \pm 78, \quad (5)$$

where the uncertainty is from U_{miss} fit.

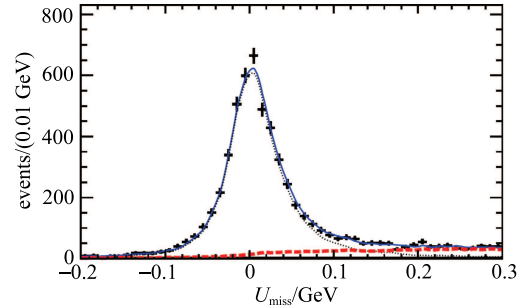


Fig. 2. (color online) Fit to the U_{miss} distribution of the $D^+ \rightarrow \bar{K}^0 e^+ \nu_e$ candidates. The dots with error bars are data, the blue solid curve is the fit result, the black dotted and the red dashed curves are the fitted signal and background.

3.3 Branching fraction

The efficiency of reconstructing the DT events, called the DT efficiency ϵ_{DT} , is determined by analyzing the signal MC events. The DT efficiencies obtained from MC simulations are corrected by the differences of π^0 reconstruction efficiencies between data and MC simulations

for the signal side. Dividing ϵ_{DT} by ϵ_{ST} , we obtain the reconstruction efficiency for $D^+ \rightarrow \bar{K}^0 e^+ \nu_e$ in each ST mode, $\epsilon_{D^+ \rightarrow \bar{K}^0 e^+ \nu_e}$, as summarized in Table 1. Weighting them by the ST yields observed in data, we obtain the averaged reconstruction efficiency of $D^+ \rightarrow \bar{K}^0 e^+ \nu_e$

$$\bar{\epsilon}_{D^+ \rightarrow \bar{K}^0 e^+ \nu_e} = (25.58 \pm 0.11)\%, \quad (6)$$

which does not include the branching fractions of $\bar{K}^0 \rightarrow \pi^0 \pi^0$ and $\pi^0 \rightarrow \gamma\gamma$.

The branching fraction of $D^+ \rightarrow \bar{K}^0 e^+ \nu_e$ is determined by

$$\begin{aligned} & \mathcal{B}(D^+ \rightarrow \bar{K}^0 e^+ \nu_e) \\ &= \frac{N_{\text{DT}}}{N_{\text{ST}}^{\text{tot}} \bar{\epsilon}_{D^+ \rightarrow \bar{K}^0 e^+ \nu_e} \mathcal{B}(\bar{K}^0 \rightarrow \pi^0 \pi^0) \mathcal{B}^2(\pi^0 \rightarrow \gamma\gamma)}, \quad (7) \end{aligned}$$

where N_{DT} is the DT yield, $N_{\text{ST}}^{\text{tot}}$ is the total ST yield, $\bar{\epsilon}_{D^+ \rightarrow \bar{K}^0 e^+ \nu_e}$ is the averaged reconstruction efficiency of $D^+ \rightarrow \bar{K}^0 e^+ \nu_e$, $\mathcal{B}(\bar{K}^0 \rightarrow \pi^0 \pi^0)$ and $\mathcal{B}(\pi^0 \rightarrow \gamma\gamma)$ are the branching fractions of $\bar{K}^0 \rightarrow \pi^0 \pi^0$ and $\pi^0 \rightarrow \gamma\gamma$ [24], respectively. Here, we assume that K_S^0 constitutes half the decays of the neutral kaons.

Inserting the numbers of N_{DT} , $N_{\text{ST}}^{\text{tot}}$, $\bar{\epsilon}_{D^+ \rightarrow \bar{K}^0 e^+ \nu_e}$, $\mathcal{B}(\bar{K}^0 \rightarrow \pi^0 \pi^0)$ and $\mathcal{B}(\pi^0 \rightarrow \gamma\gamma)$ in Eq. (7), we obtain

$$\mathcal{B}(D^+ \rightarrow \bar{K}^0 e^+ \nu_e) = (8.59 \pm 0.14)\%,$$

where the uncertainty is statistical only.

3.4 Systematic uncertainty

In the measurement of the branching fraction, the systematic uncertainty arises from the uncertainties in the fits to the M_{BC} spectra of the ST candidates, the ΔE , M_{BC} and $\bar{K}^0(\pi^0 \pi^0)$ mass requirements, the π^0 reconstruction, the e^+ tracking, the e^+ PID, the $E_{\text{max}}^{\text{extra } \gamma}$ requirement, the U_{miss} fit, the $\chi_1^2 + \chi_2^2$ selection method, the MC statistics, the quoted branching fractions and the MC generator.

The uncertainty in the fits to the M_{BC} spectra of the ST candidates is estimated to be 0.5% by observing the relative change of the ST yields of data and MC when varying the fit range, the combinatorial background shape or the endpoint of the ARGUS function. To estimate the uncertainties in the ΔE , M_{BC} and $\bar{K}^0(\pi^0 \pi^0)$ mass requirements, we examine the change in branching fractions when enlarging the ΔE selection window by 5 or 10 MeV; varying the M_{BC} selection window by ± 1 MeV/ c^2 and using alternative $\bar{K}^0(\pi^0 \pi^0)$ mass windows (0.460, 0.505), (0.470, 0.500), (0.480, 0.500) GeV/ c^2 , respectively. The maximum changes in the branching fractions, 0.3%, 0.2%, and 0.9%, are assigned as the systematic uncertainties. The π^0 reconstruction efficiency is examined by analyzing the DT hadronic decays $D^0 \rightarrow K^- \pi^+$ and $K^- \pi^+ \pi^+ \pi^-$ versus $\bar{D}^0 \rightarrow K^+ \pi^- \pi^0$ and $K_S^0(\pi^+ \pi^-) \pi^0$. The difference of the π^0 reconstruction efficiencies between data and MC is found to be

$(-1.0 \pm 1.0)\%$ per π^0 . The systematic uncertainty in π^0 reconstruction is taken to be 1.0% for each π^0 after correcting the MC efficiency of $D^+ \rightarrow \bar{K}^0 e^+ \nu_e$ to data. The data-MC differences of the e^+ tracking and PID efficiencies are estimated by analyzing $e^+ e^- \rightarrow \gamma e^+ e^-$ events. To consider different kinematic distributions of e^+ , the data-MC differences are re-weighted by the momentum and $\cos\theta$ distributions of e^+ in the $D^+ \rightarrow \bar{K}^0 e^+ \nu_e$ decays. The re-weighted data-MC difference 0.5% is quoted as the systematic uncertainties of the e^+ tracking and PID efficiencies. The uncertainty in the $E_{\text{max}}^{\text{extra } \gamma}$ requirement is estimated to be 0.1% by analyzing the DT hadronic $D\bar{D}$ decays. The uncertainty in the U_{miss} fit is assigned to be 0.5%, which is obtained by comparing with the nominal value of the branching fraction measured with an alternative signal shape obtained with different requirements on the MC-truth matched signal shape, an alternative background shape after changing the relative ratios of the dominant backgrounds (doubling each of the simulated backgrounds for $D^0 \bar{D}^0$, $D^+ D^-$ and $q\bar{q}$ continuum processes), and alternative fit range (± 50 MeV). The difference of 0.3% in the $\pi^0 \pi^0$ acceptance efficiencies of the minimum $\chi_1^2 + \chi_2^2$ requirement between data and MC, which is estimated by the DT hadronic decays $D^0 \rightarrow K^- \pi^+ \pi^0$ versus $\bar{D}^0 \rightarrow K^+ \pi^- \pi^0$, is assigned as a systematic uncertainty due to the $\chi_1^2 + \chi_2^2$ selection method. In this analysis, the $\bar{K}^0 \rightarrow K_S^0(\pi^0 \pi^0)$ mesons from the signal side are formed with photon candidates reconstructed under the assumption that they originate at the IP. We examine the DT efficiencies of the signal MC events in which the lifetimes of K_S^0 meson from the signal side are set to the nominal value and 0, respectively. The difference of these two DT efficiencies, which is less than 0.2%, is taken as the systematic uncertainty of the $K_S^0(\pi^0 \pi^0)$ reconstruction. The uncertainties in the MC statistics

Table 2. Relative systematic uncertainties (in %) in the measurement of $\mathcal{B}(D^+ \rightarrow \bar{K}^0 e^+ \nu_e)$.

source	uncertainty
M_{BC} fit	0.5
ΔE requirement	0.3
$M_{\text{BC}} \in (1.863, 1.877)$ GeV/ c^2	0.2
$M_{\pi^0 \pi^0} \in (0.45, 0.51)$ GeV/ c^2	0.9
π^0 reconstruction	2.0
tracking for e^+	0.5
PID for e^+	0.5
$E_{\text{max}}^{\text{extra } \gamma} < 0.3$ GeV	0.1
U_{miss} fit	0.5
$\chi_1^2 + \chi_2^2$ selection method	0.3
$K_S^0(\pi^0 \pi^0)$ reconstruction	0.2
MC statistics	0.5
$\mathcal{B}(\bar{K}^0 \rightarrow \pi^0 \pi^0)$	0.2
MC generator	0.1
total	2.5

and the $\mathcal{B}(\bar{K}^0 \rightarrow \pi^0\pi^0)$ are 0.5% and 0.2% [24], respectively. In our previous work, the uncertainty in the signal MC generator is estimated to be 0.1%, which is obtained by comparing the DT efficiencies before and after re-weighting the $q^2(= (p_D - p_K)^2)$ distribution of the signal MC events of $D^0 \rightarrow K^- e^+ \nu_e$ to the distribution found in data [11], where the p_D and p_K are the four-momenta of the D and K mesons. The systematic uncertainties are summarized in Table 2. Adding all uncertainties in quadrature, we obtain the total systematic uncertainty to be 2.5%.

3.5 Validation

The analysis procedure is examined by an input and output check using an inclusive MC sample equivalent

to a luminosity of 3.26 fb^{-1} . Using the same selection criteria as those used in data analysis, we obtain the ST yield, the DT yield and the weighted reconstruction efficiency of $D^+ \rightarrow \bar{K}^0 e^+ \nu_e$ to be 1683631 ± 1768 , 5802 ± 85 and $(26.07 \pm 0.11)\%$, where no efficiency correction has been performed. Based on these numbers, we determine the branching fraction $\mathcal{B}(D^+ \rightarrow \bar{K}^0 e^+ \nu_e) = (8.82 \pm 0.13)\%$, where the uncertainty is statistical only. The measured branching fraction is in excellent agreement with the input value of 8.83%.

To validate the reliability of the MC simulation, we examine the $\cos\theta$ and momentum distributions of \bar{K}^0 and e^+ of the $D^+ \rightarrow \bar{K}^0 e^+ \nu_e$ candidates, as shown in Fig. 3. We can see that the consistency between simulation and data is very good.

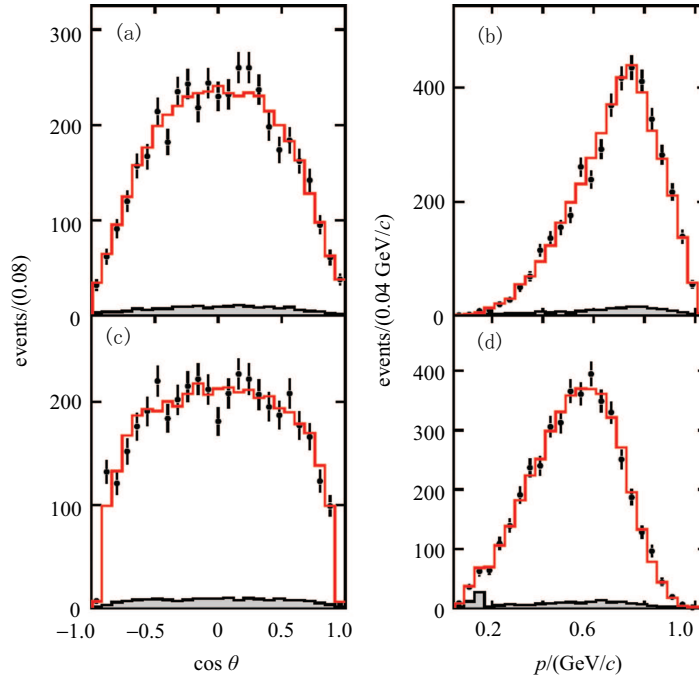


Fig. 3. (color online) Comparisons of the $\cos\theta$ and momentum distributions of \bar{K}^0 ((a), (b)) and e^+ ((c), (d)) of the $D^+ \rightarrow \bar{K}^0 e^+ \nu_e$ candidates. The dots with error bars are data, the red histograms are the inclusive MC events, and the light black hatched histograms are the MC simulated backgrounds. These events satisfy a tight requirement of $-0.06 \text{ GeV} < U_{\text{miss}} < +0.06 \text{ GeV}$.

4 Summary and discussion

Based on the analysis of 2.93 fb^{-1} data collected at $\sqrt{s} = 3.773 \text{ GeV}$ with the BESIII detector, we measure the absolute branching fraction $\mathcal{B}(D^+ \rightarrow \bar{K}^0 e^+ \nu_e) = (8.59 \pm 0.14 \pm 0.21)\%$, using $\bar{K}^0 \rightarrow K_S^0 \rightarrow \pi^0\pi^0$. Figure 4 presents a comparison of $\mathcal{B}(D^+ \rightarrow \bar{K}^0 e^+ \nu_e)$ measured in this work with the results obtained by other experiments. Our result is well consistent with the other measurements within uncertainties and has a precision comparable to the PDG value [24]. Our measurement will be helpful

to improve the precision of the world average value of $\mathcal{B}(D^+ \rightarrow \bar{K}^0 e^+ \nu_e)$.

Combining the PDG values for $\mathcal{B}(D^0 \rightarrow K^- e^+ \nu_e)$, $\mathcal{B}(D^+ \rightarrow \bar{K}^0 e^+ \nu_e)$ [24], and the lifetimes of D^0 and D^+ mesons (τ_{D^0} and τ_{D^+}) [24] with the value of $\mathcal{B}(D^+ \rightarrow \bar{K}^0 e^+ \nu_e)$ measured in this work, we determine

$$\frac{\Gamma(D^0 \rightarrow K^- e^+ \nu_e)}{\Gamma(D^+ \rightarrow \bar{K}^0 e^+ \nu_e)} = \frac{\mathcal{B}(D^0 \rightarrow K^- e^+ \nu_e) \times \tau_{D^0}}{\mathcal{B}(D^+ \rightarrow \bar{K}^0 e^+ \nu_e) \times \tau_{D^+}} = 0.969 \pm 0.025, \quad (8)$$

where $\bar{\mathcal{B}}(D^+ \rightarrow \bar{K}^0 e^+ \nu_e)$ is the uncertainty averaged

branching fraction based on the PDG value and the one measured in this work. Combining with the branching

fraction measured in this work, the precision of the test of the isospin symmetry is improved.

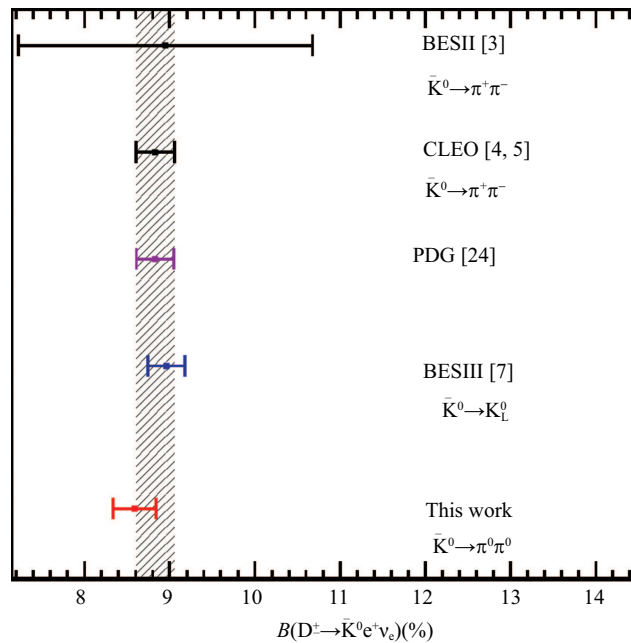


Fig. 4. (color online) Comparison of the $\mathcal{B}(D^+ \rightarrow \bar{K}^0 e^+ \nu_e)$ measured in this work with those measured by other experiments, where the slash band is the world averaged branching fraction with uncertainty. For the BESIII measurement using $\bar{K}^0 \rightarrow K_L^0$, we take $\mathcal{B}(D^+ \rightarrow \bar{K}^0 e^+ \nu_e) = 2\mathcal{B}(D^+ \rightarrow K_L^0 e^+ \nu_e)$.

The BESIII collaboration thanks the staff of BEPCII

and the IHEP computing center for their strong support.

References

- 1 Y. Fang, G. Rong, H. L. Ma, and J. Y. Zhao, *Eur. Phys. J. C*, **75**: 10 (2015)
- 2 Z. Bai et al (MARKIII Collaboration), *Phys. Rev. Lett.*, **66**: 1011 (1991)
- 3 M. Ablikim et al (BES Collaboration), *Phys. Lett. B*, **608**: 24 (2005)
- 4 D. Besson et al (CLEO Collaboration), *Phys. Rev. D*, **80**: 032005 (2009)
- 5 J. Y. Ge et al (CLEO Collaboration), *Phys. Rev. D*, **79**: 052010 (2009)
- 6 M. Ablikim et al (BESIII Collaboration), *Study of dynamics of $D^+ \rightarrow \bar{K}^0(\pi^+\pi^-)e^+\nu_e$ and $D^+ \rightarrow \pi^0 e^+\nu_e$ decays*, publication in preparation
- 7 M. Ablikim et al (BESIII Collaboration), *Phys. Rev. D*, **92**: 112008 (2015)
- 8 M. Ablikim et al (BESIII Collaboration), *Chin. Phys. C*, **37**, 123001 (2013)
- 9 M. Ablikim et al (BESIII Collaboration), *Phys. Lett. B*, **753**: 629 (2016)
- 10 M. Ablikim et al (BESIII Collaboration), *Nucl. Instrum. Methods A*, **614**: 345 (2010)
- 11 M. Ablikim et al (BESIII Collaboration), *Phys. Rev. D*, **92**: 072012 (2015)
- 12 S. Agostinelli et al (GEANT4 Collaboration), *Nucl. Instrum. Methods A*, **506**: 250 (2003)
- 13 S. Jadach, B. F. L. Ward, and Z. Was, *Comp. Phys. Commu.*, **130**: 260 (2000)
- 14 S. Jadach, B. F. L. Ward, and Z. Was, *Phys. Rev. D*, **63**: 113009 (2001)
- 15 E. Barberio and Z. Was, *Comput. Phys. Commu.*, **79**: 291 (1994)
- 16 E. A. Kureav and V. S. Fadin, *Sov. J. Nucl. Phys.*, **41**: 466 (1985) [*Yad. Fiz.*, **41**: 733 (1985)]
- 17 D. J. Lange, *Nucl. Instrum. Methods A*, **462**: 152 (2001)
- 18 R. G. Ping, *Chin. Phys. C*, **32**: 599 (2008)
- 19 K. Nakamura et al (Particle Data Group), *J. Phys. G*, **37**: 075021 (2010) and 2011 partial update for the 2012 edition
- 20 J. C. Chen, G. S. Huang, X. R. Qi et al, *Phys. Rev. D*, **62**: 034003 (2000)
- 21 D. Becirevic and A. B. Kaidalov, *Phys. Lett. B*, **478**: 417 (2000)
- 22 J. Adler et al (MARKIII Collaboration), *Phys. Rev. Lett.*, **62**, 1821 (1989)
- 23 K. T. Chao and Y. F. Wang, *Physics at BESIII*, p. 38-40
- 24 K. A. Olive et al (Particle Data Group), *Chin. Phys. C*, **38**: 090001 (2014)
- 25 X. Ma, Z. P. Mao, J. M. Bian et al, *Chin. Phys. C*, **32(9)**: 744 (2008)
- 26 H. Albrecht et al (ARGUS Collaboration), *Phys. Lett. B*, **241**: 278 (1990)